

# Multishading masks: a new method for assessing solar penetration in open spaces

RAPHAËL COMPAGNON, JOËLLE GOYETTE-PERNOT

University of Applied Sciences of Western Switzerland (HES-SO)  
Fribourg College of Engineering and Architecture (EIA-FR)  
Bd. Pérolles 80, 1705 Fribourg, Switzerland  
e-mail : raphael.compagnon@hefr.ch & joelle.goyette@hefr.ch

*ABSTRACT: So called “multishading masks” are obtained by combining together several shading masks computed for a series of sample points uniformly distributed over the open space under study. By superimposing these “multishading masks” with common sun-path diagrams, it is possible to assess which area fraction of an open space is exposed to sunlight during the different seasons and to verify if additional shading elements (e.g. trees) can improve users’s satisfaction. When combined with sky radiance distributions, the same “multishading masks” can also be used to quantify irradiance levels reaching open spaces.*

*Keywords: solar access, open spaces, shading masks, irradiance levels, computer tool*

## INTRODUCTION

It is well known that sunlight is highly appreciated in open spaces. However, when built in urban locations, the solar access of these open spaces is usually largely affected by the surrounding buildings. Hence, some legal requirements are set by planning authorities. For instance this article extracted from a local law about country planning: “Children playgrounds must be located off traffic and benefit from sufficient sunlight” [1]. The question immediately arises to know which measurable characteristics have to be used to check to which level a design proposal meets such a requirement.

From comfort field studies in open spaces, it appears that their users’ satisfaction is also enhanced as long as some shaded areas are provided [2, 3]. How is it possible to ensure that an appropriate proportion of shaded/sunlit areas is available throughout the year on a planned open space?

These two above examples illustrate the need for an appropriate tool to assess sunlight penetration in open spaces using clearly defined criteria. Shading masks due to surrounding obstructions superimposed on sun-path diagrams are commonly used to evaluate solar access for single punctual locations [4]. However, for studying an open space as a whole area, these projections do not provide much help since they differ considerably from one point to another.

The new method presented hereafter is devised to overcome this problem. It is also based on a projection

of the sky vault. However, instead of being calculated for a single point, it combines the projections calculated for many sample points located on a regular grid that covers the whole area of interest. Hence the name “multishading masks” given to the resulting projection that eventually appears as a defocused view of the surrounding obstructions.

## FROM SHADING TO MULTISHADING MASKS

Computer tools calculating shading masks for outdoor locations in built environments are already available and often used to characterize sunlight penetration and to evaluate sky view factors as important parameters required to assess the local microclimate and the resulting thermal comfort conditions [5, 6]. Usually these tools compute shading masks for punctual locations.

The shading mask for a punctual location numbered  $k$  is defined as a function  $vis(p,k)$  where  $p$  is indexing all the tiny patches by which the entire sky vault hemisphere is subdivided. The  $vis(p,k)$  function aims to characterize the visibility between sky patch  $p$  and point  $k$ ; it is equal to 1 if a light ray coming from sky patch  $p$  is reaching point  $k$  without any obstruction and 0 otherwise. When a digital 3D model of the studied area is available, this function is typically evaluated using a ray-tracing algorithm. Hemispherical or stereographic projections are then commonly used to represent  $vis(p,k)$  as pictures with obstructed sky regions coloured in black and, conversely, unobstructed sky regions coloured in

white or kept transparent. These are later superimposed on a sun-path diagram in order to determine the time periods for which sunlight can reach or not the studied point.

A rectangular courtyard enclosed by 4 to 5 storeys' buildings is used here as an application example (urban block surrounded by Feldbergstrasse-Hammerstrasse-Halteringerstrasse-Riehenring in Basel, Switzerland). Shading masks have been calculated using a 3D digital model of this building block processed using the RADIANCE lighting simulation software [7]. As shown on Fig. 1, these shading masks differ considerably among different selected points spread across the large open space located inside the courtyard (e.g. a recreative garden). Thus, if the analysis is conducted in order to assess the sunlight penetration for this garden performing as a single entity, these shading masks unfortunately don't provide much help. For which reason should one of these points (A, B or C) or any other one located in the garden be considered as representative of the sunlight access of the whole area? One possible answer is to assume that the users of this garden will stay at one specific place most of the time.

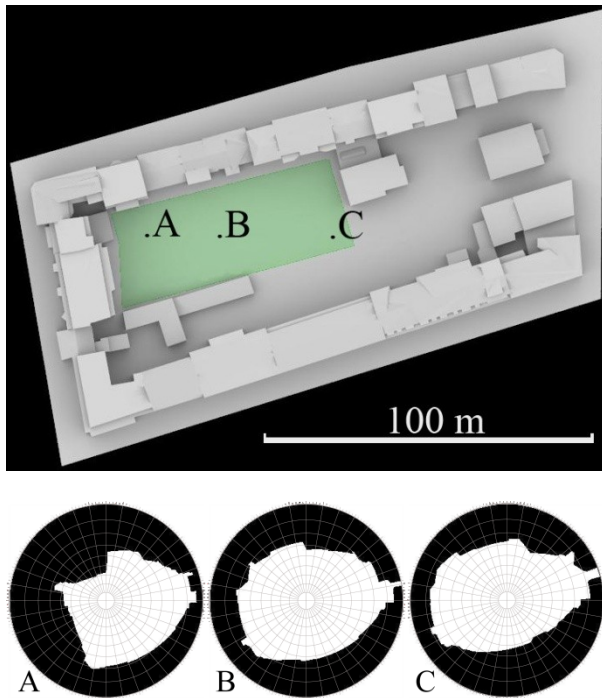


Figure 1: Above: plan view of the courtyard used as an application example. The green area (1952 [m<sup>2</sup>]) highlights the garden for which solar access is analysed. Below: shading masks computed for points A, B and C.

However, when the users have free access to the whole area, it is reasonable to assume that, beside many other reasons, they will also change their position in

order to increase their satisfaction with thermal comfort. Depending on the other factors affecting thermal comfort (e.g. air temperature, wind speed, metabolic activity, clothing level) a position either in shade or sunlight will be preferred. Therefore, it can be admitted that an open space will be better perceived if shaded and sunlit areas are simultaneously present at all times so that users can always make their own choice.

In order to easily check this requirement, the proposed method is simply to superimpose several shading masks into a single new one called a "multishading mask". To achieve this, a series of N uniformly distributed sample points are first positioned over the open space under study. Typically, these points are located 1.1 [m] above ground level (i.e. centre of gravity height of a standing person) and spaced together by ~1 [m]. Then for each sky patch p the following mean is computed over the N sample points indexed by k:

$$M_p = N^{-1} \cdot \sum_{k=1}^N \text{vis}(p, k) \quad \text{in } [-]$$

where vis(p,k) is the same visibility function as defined previously.

The  $M_p$  values are comprised between 0 and 1. In fact they are indicating the area fraction of the whole open space that is unobstructed toward each sky patch p. Finally, the so called "multishading mask" can be produced as a picture (in hemispherical or stereographical projection) where each pixel refers to a particular sky patch p and shows its  $M_p$  value mapped on a linear gray level scale going from black ( $M_p=0$  i.e. a sky patch that is totally obstructed over the whole area) to white ( $M_p=1$  i.e. a sky patch that is totally unobstructed over the whole space) (Fig. 2).

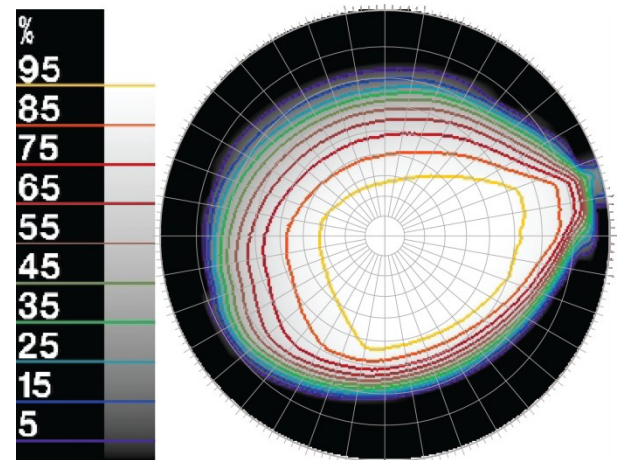


Figure 2: Multishading mask computed for the garden. The  $M_p$  values are expressed in % (scale on the left) and coloured iso-value lines have been superimposed.

It must be noted that multishading masks as defined above are similar to “cumulative shading” masks generable by the ECOTECT software [8]. In fact these diagrams show the fraction of an open space that every part of the sky can freely “see”.

### INTERPRETING MULTISHADING MASKS

Once a multishading mask is available for an open space, it can be used to precisely evaluate its solar access. One important criterion is to check the simultaneous availability of shaded and sunlit areas. In order to ensure that both these areas can play a true role for the users, they should at least cover a significant percentage of the open space. In this paper this limit is arbitrarily fixed to 20% but the proposed method could accommodate any other limit as well.

The multishading mask can then be processed to highlight the sky zones for which the above criterion is met or not. This is done by colouring the mask using the following rules:

- yellow colour for “overlighting” zones (i.e.  $M_p \geq 80\%$ );
- green colour for “overshading” zones (i.e.  $0 < M_p \leq 20\%$ ).

The remaining sky zones are those that are either totally obstructed for the whole site ( $M_p=0$ ; coloured in black) or those coloured with levels of gray for which the criterion is met (i.e.  $20\% < M_p \leq 80\%$ ). A sun-path diagram for the location is then superimposed (Fig. 3).

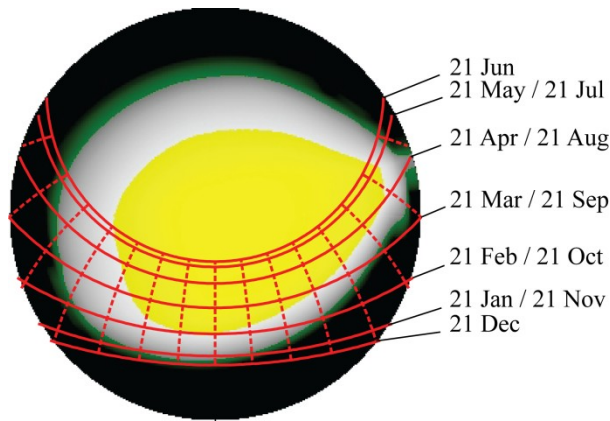


Figure 3: Processed multishading mask computed for the garden. The sun-path for Basel city’s latitude ( $47.6^\circ N$ ) is superimposed (dotted lines indicate hours in true solar time).

The resulting interpretation is straightforward: the red sun-path lines cross the yellow “overlighting” sky zone for several hours each day (from  $\sim 2$  hours at end of February to  $\sim 10$  hours in June and back to  $\sim 2$  hours until the end of October). This means that this garden is overexposed to sunlight during this long period. From end of October to end of November as well as from end

of January to end of February, the red sun-path curves entirely remain in the gray coloured zone for respectively  $\sim 6.5$  and  $\sim 2.5$  hours a day. This indicates that the garden is adequately sunlit (at least according to the criterion defined previously) for this month interval. The remaining winter period (end of November to end of January), because of the southern buildings’ row, the garden clearly suffers from a lack of sunlight.

From this analysis it appears that some kind of additional shadowing elements (e.g. trees, pergola, and awning) should be added around or inside de garden in order to decrease or even eliminate the yellow “overlighting” zone on the multishading mask. As such an example, a row comprising five large trees is supposed to be located in the garden. The trees are here simply added to the 3D model of the site as spherical opaque objects with 4.5 [m] radius centred 7 [m] above ground level. Two alternate cases for the trees row’s location are studied (Fig. 4).

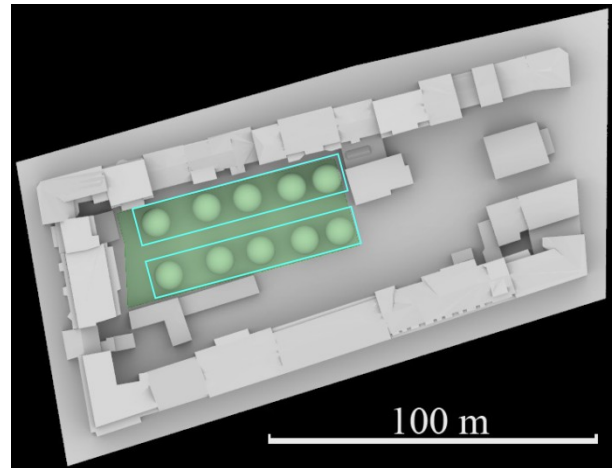


Figure 4: Two proposals for supplementary shading elements: a row of 5 big trees planted either along the garden’s northern edge (close to the buildings) or along its southern edge.

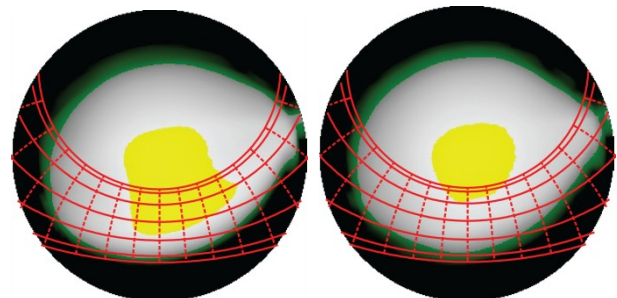


Figure 5: Processed multishading masks computed for the garden with a row comprising five big trees. Left: with trees located along garden’s northern edge. Right: with trees located along garden’s southern edge. The sun-path for Basel city’s latitude ( $47.6^\circ N$ ) is superimposed (dotted lines indicate hours in true solar time).

As shown on Fig. 5, the multishading masks computed for these two cases appear very different: from beginning of spring to the end of summer the garden remain overexposed to sunlight for 3 to 4.5 hours a day when the trees are located on the garden’s northern edge (Fig 5, left). Conversely, when the trees are located on the garden’s southern edge, the overexposed period is significantly reduced from the end of April to the end of August (Fig 5, right). In the winter months from mid- November to mid-February, the overshading effect is more pronounced when the trees are located on the southern edge. However, during this season, deciduous trees have lost their foliage and their shading effect is thus overestimated by our model which assumes totally opaque trees.

### QUANTIFYING IRRADIANCE LEVELS WITH MULTISHADING MASKS

Multishading masks can also serve to assess the mean irradiance level (noted  $I$ ) received by an open space. For this purpose, all sky patches (indexed by  $p$ ) must be summed together using equation:

$$I = \sum_p (M_p \cdot \omega_p \cdot R_p) \quad \text{in } [W \cdot m^{-2}]$$

with:

- $M_p$  (in [-]): the multishading mask value for sky patch  $p$
- $\omega_p$  (in [sr]): the projected solid angle (relative to the ground horizontal plane) of sky patch  $p$
- $R_p$  (in [ $W \cdot sr^{-1} \cdot m^2$ ]): the radiance value of sky patch  $p$

It is important to note that the irradiance computed by this equation accounts the diffuse and direct radiation coming from the sky vault only; i.e. the diffuse radiation component reflected by the ground and the surrounding obstructions is not accounted! To perform this calculation, a distribution of the mean radiance values  $R_p$  calculated over the entire sky vault for a determined time interval is required. Here we make use of an annual statistical sky model computed as described in [9] for Basel city from a set of diurnal hourly weather data (4124 hours) of a full year obtained using the METEONORM software [10].

Table 1 shows the mean global irradiance values computed for our examples. As expected, the lowest mean irradiance is observed for the better shaded case (garden with trees planted along its southern edge).

The three terms product inside this equation can also be easily visualized by superimposing three diagrams (i.e. this is done by multiplying their pixel values). The mean irradiance level  $I$  can be intuitively perceived by the overall brightness of the resulting “product picture” (Fig. 6). Thus, even without performing any real calculations, quantitative comparisons can be made

between various designs just by superimposing their respective multishading masks  $M_p$  with the projected solid angle distribution  $\omega_p$  and the sky radiance distribution  $R_p$  for the desired location.

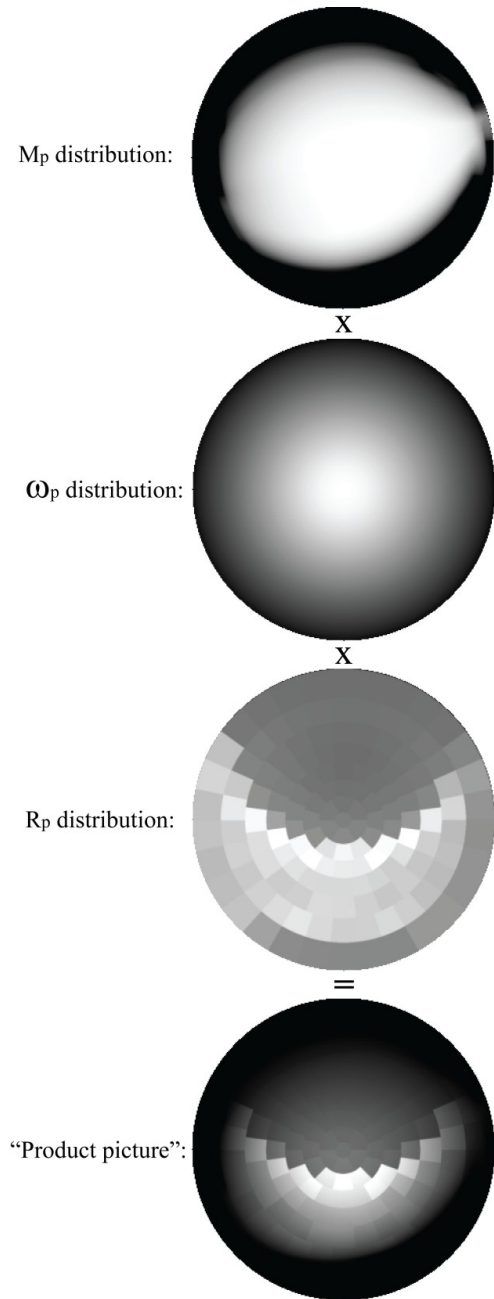


Figure 6: Calculation of a “product picture” (bottom) by multiplying each corresponding pixel of three pictures showing respectively:

- the  $M_p$  distribution (i.e. the multishading mask) computed here for the empty garden;
- the  $\omega_p$  distribution (i.e. the projected solid angle of each sky patch);
- the  $R_p$  distribution (i.e. the sky radiance values).

All these pictures have been mapped on arbitrary linear gray level scales.

Table 1: Mean global irradiance values computed for our examples and an imaginary totally unobstructed site (Basel city annual sky model comprising 4124 diurnal hours).

Case	I [Wm <sup>-2</sup> ]	Δ
empty garden (reference)	208	0
garden with trees on North	170	-18 %
garden with trees on South	157	-25 %
unobstructed site	262	+26 %

## CONCLUSION

The multishading mask method presented in this paper offers a practical tool to easily assess sunlight penetration in open spaces already at the design stage as long as a digital 3D model of the surrounding buildings is available. Analysing multishading masks is a straightforward task since it can be performed graphically by superimposing them on common sun-path diagrams to estimate the duration either of over- or under- exposition to sunlight. Furthermore, by superimposing multishading masks with sky radiance distributions calculated for specific sites, they can serve to quantitatively estimate the mean irradiance received by an open space. Applications of the method in various fields can be anticipated, e.g:

- outdoor thermal comfort: to ascertain that a proposed design for an open space will simultaneously provide shaded and sunlit areas in adequate proportions;
- rights to sunlight: to precisely quantify the loss of sunlight exposure on an existing open space when a new construction is planned in its immediate surrounding or, conversely, to quantify the increase of sunlight exposure expected from a demolition;
- detailed planning of an open space: to compare alternate layouts for locating various zones and equipments typical of an open space (e.g. children playground, benches, sport installations, water pond) or to ascertain if a selected vegetation type will get an adequate irradiance level to grow satisfactorily;
- architecture and urban planning education: to clearly illustrate courseware and to train students on solar access issues. For this purpose, a series of pre-computed multishading masks can be prepared for open spaces surrounded by typical building layouts (e.g. urban canyons or courts of various height/width ratios) as well as sun-path and sky radiance distributions diagrams for selected climates. After printing these masks and diagrams on transparent sheets, various didactic experiments can be performed by

students simply by superimposing the appropriate sheets!

By now the multishading mask calculation and analysis tools are implemented as specific programs built around modules of the RADIANCE lighting simulation software installed on UNIX/LINUX systems [7]. Before we could assemble these tools into an interactive internet online service as we foresee, we are ready to share them with some interested academic users.

## ACKNOWLEDGEMENTS

This work was first carried out in 2003 within the RUROS project [11]. It was developed further by the main author while working as a visiting scientist at the Solar Energy Research Institute of Singapore (SERIS) in 2012 and is currently being used within a research project on sustainable neighborhoods (ATEQUAS project). Marylène Montavon kindly provided us the 3D digital model of the building block used as an example.

## REFERENCES

1. Etat de Fribourg, (2009). Règlement d'exécution de la loi sur l'aménagement du territoire et les constructions (ReLATeC), Art. 63. [Online], Available : <http://bdlf.fr.ch/frontend/versions/2439> [3 May 2013].
2. Nikolopoulou, M., Lykoudis, S., (2006). Thermal comfort in outdoor urban spaces: Analysis across different European countries. *Building and Environment*, 41(11), pp. 1455-1470.
3. Nikolopoulou, M., Baker, N., Steemers, K., (2001). Thermal comfort in outdoor urban spaces: understanding the human parameter. *Solar Energy*, 70(3), pp. 227-235.
4. Littlefair, P.J. et al., (2000). Environmental Site Layout Planning: Solar Access, Microclimate and Passive Cooling in Urban Areas, BRE Report BR 380, Building Research Establishment, Garston.
5. Teller, J., Azar, S., (2001). Townscope II - A computer system to support solar access decision-making. *Solar Energy*, 70(3), pp. 187-200.
6. Gulyás, A., Unger, J., Matzarakis, A., (2006). Assessment of the microclimatic and human comfort conditions in a complex urban environment: Modelling and measurements. *Building and Environment*, 41(12), pp. 1713-1722.
7. RADSITE, Radiance software and users' community homepage, [Online], Available: <http://radiance-online.org> [3 May 2013].
8. Ecotect Community Wiki. Partial shading. [Online], Available: [http://wiki.naturalfrequency.com/wiki/Partial\\_Shading](http://wiki.naturalfrequency.com/wiki/Partial_Shading) [3 May 2013].
9. Compagnon, R., (2004). Solar and daylight availability in the urban fabric. *Energy and Buildings* 36(4), pp. 321-328.
10. METEONORM software homepage. [Online], Available: <http://meteonorm.com> [3 May 2013].
11. RUROS project homepage, Rediscovering the Urban Realm and Open Spaces, [Online], Available: <http://alpha.cres.gr/ruros/> [3 May 2013].